УДК 539.1, 0.74.2;
51-72: 539.12

SIMULATION RESULTS AND SUGGESTIONS FOR POSSIBLE DESIGN OF GASEOUS SHOWER MAXIMUM DETECTOR FOR THE ENDCAP ELECTROMAGNETIC CALORIMETER FOR THE STAR EXPERIMENT AT RHIC

G.Averichev, S.Chernenko, E.Matyushevskiy, Yu.Minaev, Yu.Panebratsev, E.Potrebenikova, D.Razin, S.Razin, L.Smykov, G.Škoro, A.Shabunov, I.Tsvetkov, V.Yurevich, Yu.Zanevskiy

The Monte Carlo simulation of Shower Maximum Detector (SMD) for the endcap EMC has been performed for *pp*, *p*Au and AuAu collisions. A conceptual design of gaseous SMD with a pad readout of signals is proposed.

The investigation has been performed at the Laboratory of High Energies, JINR.

Моделирование и возможные реализации газового детектора максимума ливня торцевого электромагнитного калориметра установки STAR на ускорителе RHIC

Г.Аверичев и др.

Проведено моделирование детектора максимума ливня торцевого электромагнитного калориметра для *pp*, *p*Au и AuAu столкновений. Предложен газовый детектор максимума ливня с катодной плоскостью, имеющей pad-структуру.

Работа выполнена в Лаборатории высоких энергий ОИЯИ.

1. Introduction

In our previous report [1] we presented the results of Monte Carlo simulations of endcap EMC Shower Maximum Detector (SMD) for the STAR and experimental investigations of characteristics of the Russian tiny photomultipliers PMT in order to specify their applicability in the SMD. Our results show that the scintillator strip/fiber SMD is good option for the endcap SMD in the case of *pp* and *p*Au collisions. Application of Russian tiny PMT with low gain allows us to build relatively low-cost SMD with low number of high voltage supply channels. But, one of the most important conclusions of our previous work [1] was that this type SMD is not suited for the job in the AuAu collision case. In what follows, we present results of our MC calculations and main ideas about the conceptual design of SMD for endcap EMC with a pad readout of signals.

2. Monte Carlo Simulations

2.1. *SMD Parameters.* The CERN Monte Carlo program GEANT3.15 with a 1 MeV cut for γ's and electrons was used to study EM showers for full STAR detector, and HIJING model event generator has been used for describing of proton-nucleus and nucleus-nucleus collisions.

During the MC simulations the SMD was placed at the depth of $5X_0$ in the endcap EMC and consisted of two scintillation rings (inner radius — 75 cm, outer radius — 232 cm, thickness — 6 mm).

In Fig.1 the pseudorapidity distributions of γ's and charged hadrons in *pp*, *p*Au and AuAu collisions are presented. The distributions of energies for direct gammas and gammas from π^0 decays in acceptance of the endcap EMC are shown in the right side of this picture. The number of γ's in the SMD acceptance is about 800 for central AuAu collision and about 10 in central *p*Au collision.

Scatter plot of shower charged particles distribution on the first SMD layer is presented in Fig.2a. In Fig.2b we show the number of this particles as a function of the distance R from the SMD centre. It is seen that about 75% of showers, produced in the interactions of primary γ's (about 600) with the calorimeter matter, lie in the central ($75 < R < 160$ cm) SMD region.

The same distributions for the primary gammas with energy above 500 MeV are presented in Fig.3. Comparison of Fig.2 and Fig.3 tells us that the contribution of showers, induced by gammas with energy lower than 500 MeV, is practically negligible, and we can conclude that the main sources of background (for observation of direct γ's) are hadrons and gammas with energy higher than 500 MeV.

Figure 4 shows the transverse profiles of shower, induced by 15 GeV gamma on the middle part of the first and second layer of SMD at the pseudorapidity $\eta \simeq 1.5$. RMS of the shower transverse profiles is about 2.3 cm. This means that the granularity of the SMD must be better than 10—12 mm for both layers in order to identify and separate the showers. The IHEP group experimental data [2] confirm our conclusion.

To obtain a uniform deposited energy over full surface of SMD layer, we have account for dependence of deposited energy on the radius R in the central SMD region ($75 < R < 160$) cm. We can see that for $R > 160$ cm deposited energy practically does not depend on the distance R. The data for the central SMD region were used for the fitting procedure and the fitted function was of the form $\Delta E = a + b \cdot R$. The results of the fit were used to determine the width of the inner ring strips, taking into account that the widths of outer strips are equal to $\Delta R = 12$ mm. The total number of ring strips defined in such manner is 190. The total width of the central ring strip is 4 mm.

The next step was a determination of a number of strips in the azimuthal direction and, as a result, we have practically defined the pad structure of the SMD layer. In Fig.5 is shown the energy deposited in the central 6 cm width ring of SMD vs. azimuthal angle for 6°, 3° and 1° per bin for the central AuAu collision. The width of 6 cm corresponds to the full width at 1/10 th of maximum height of the shower transverse profile. The 1° azimuthal angle bin corresponds to the geometrical size of ~13 mm in the central part of SMD and using these pads we can clearly identify the single shower. Referring to Fig.5a and Fig.5b one sees that all showers are separated with the 3° azimuthal angle widths pads. Finally, the proposed pad structure of the first SMD plane gives us the possibility of separating showers

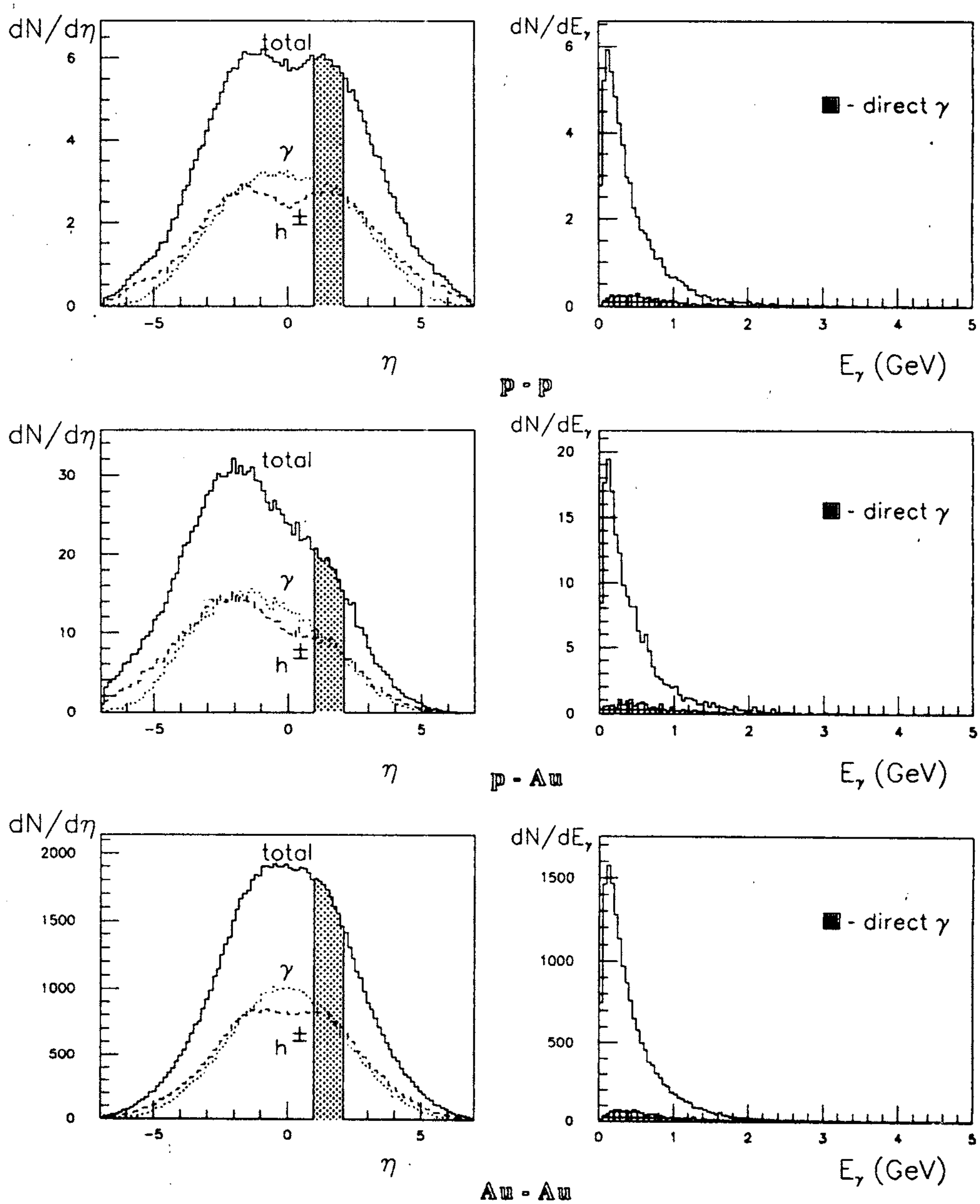

Fig.1. The pseudorapidity distribution of γ's and charged hadrons in *pp*, *p*Au and AuAu collisions at 200 GeV/nucelon

in the central SMD region using the information about two coordinates (*R* and φ). But we would like to point out that for separating the showers in the outer part of the SMD the information about φ coordinate from the second plane (wires or strip with 10 mm step, for example) is needed.

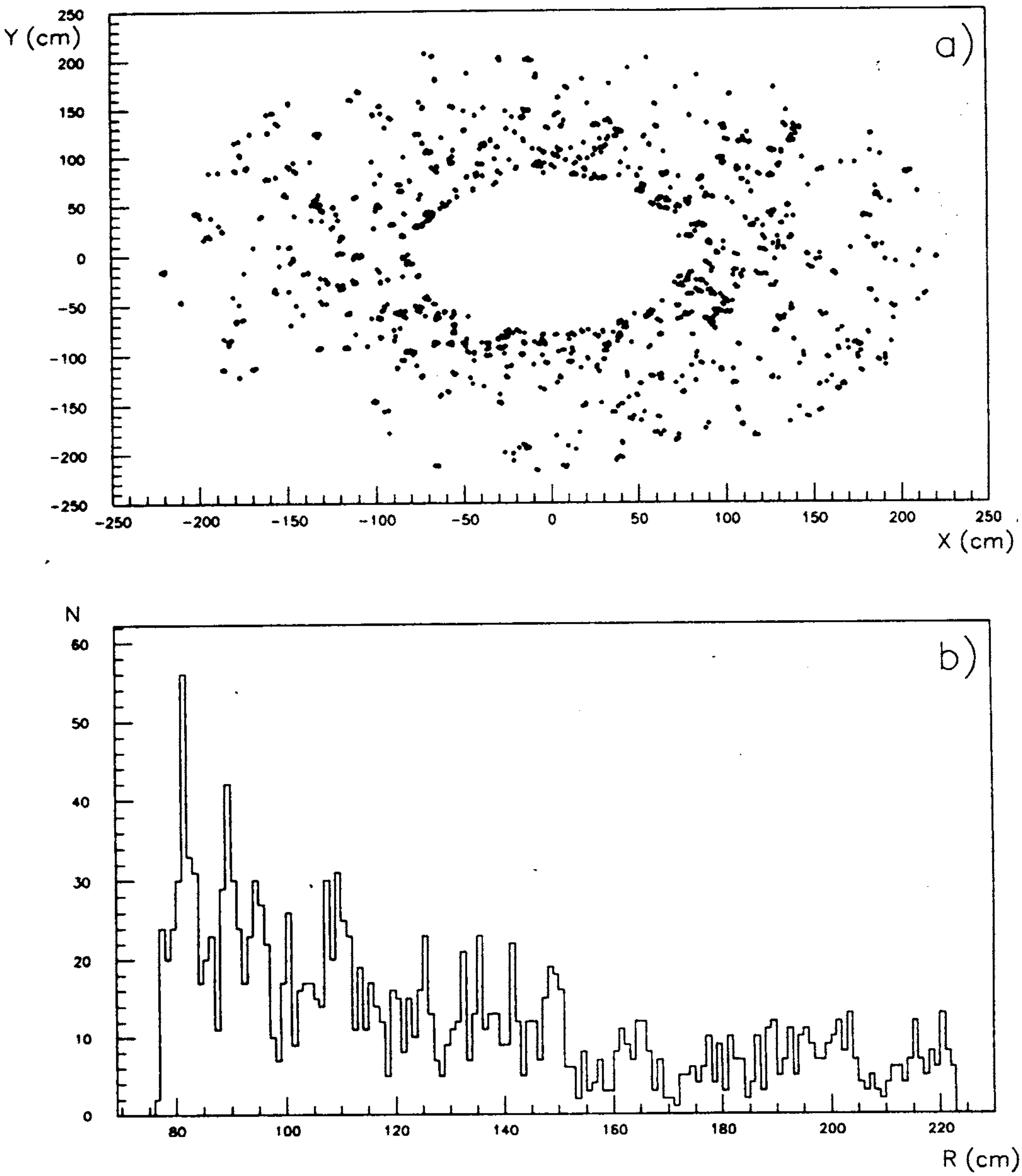

Fig.2. (a) Scatter plot of shower charged particles distribution on the first SMD layer; (b) The number of shower charge particle vs. the distance from the SMD centre

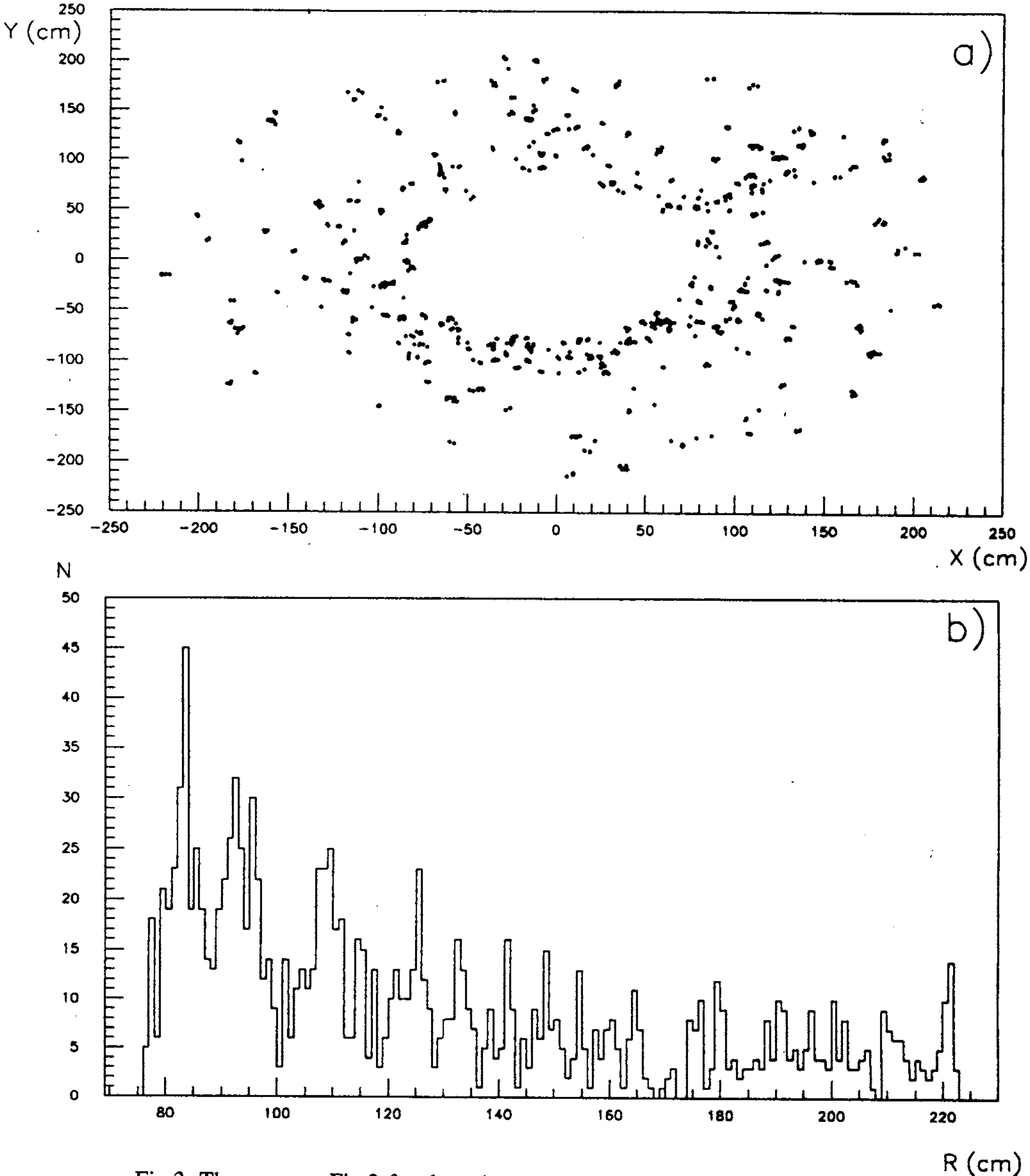

Fig.3. The same as Fig.2 for the primary γ's with energy above 500 MeV

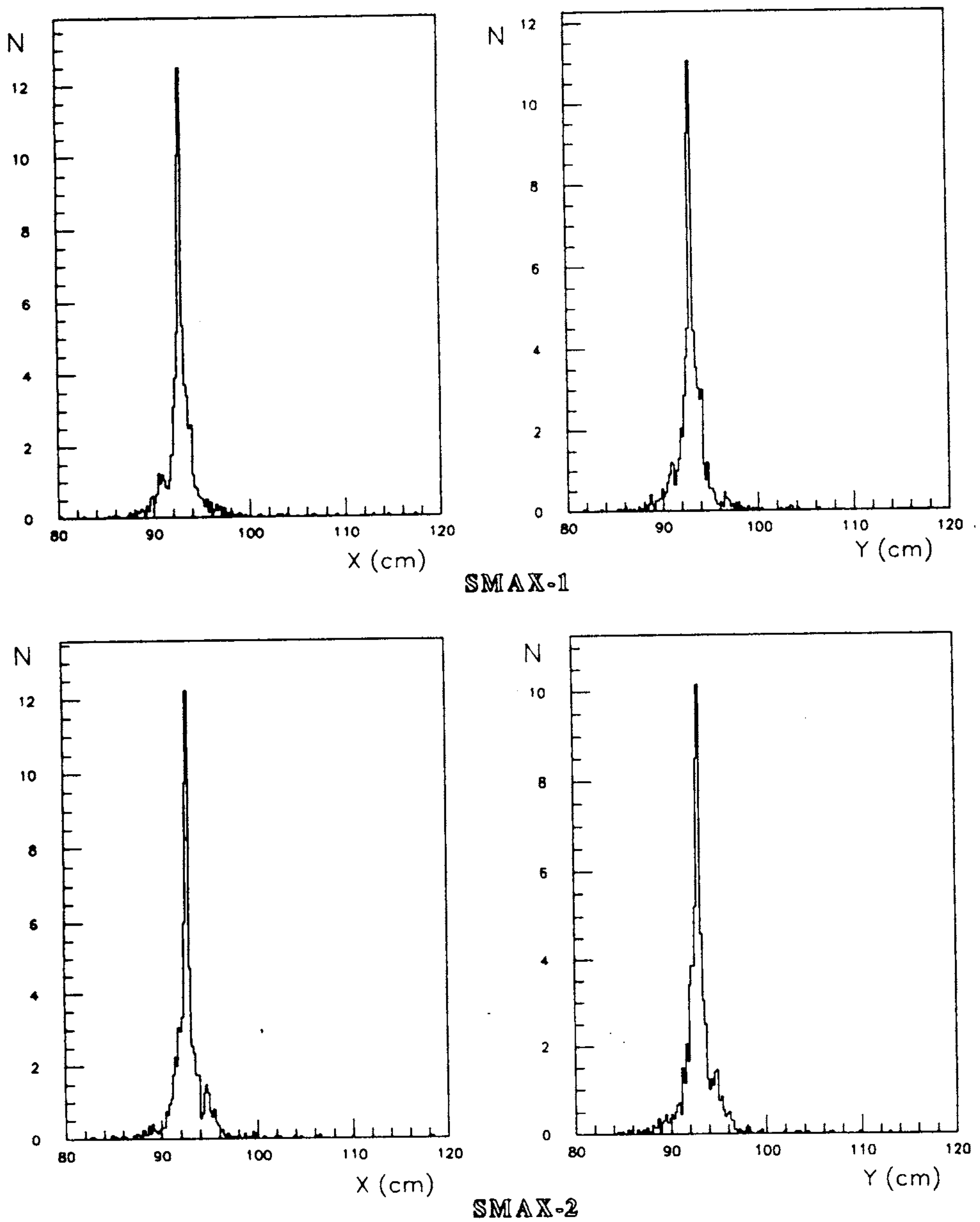

Fig.4. The transverse profiles of shower, induced by 15 GeV gamma

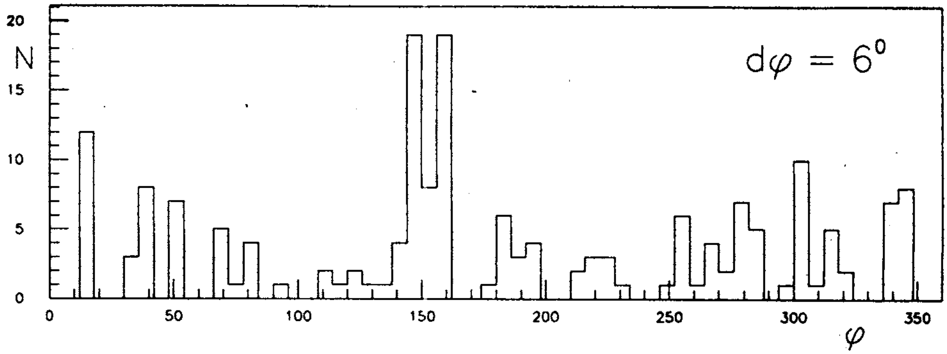

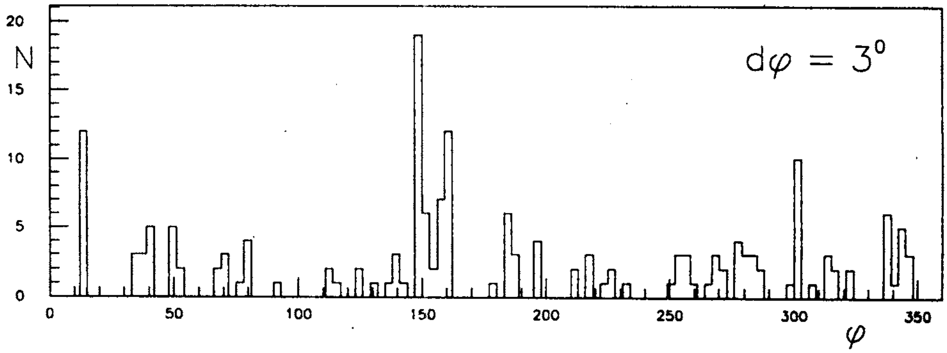

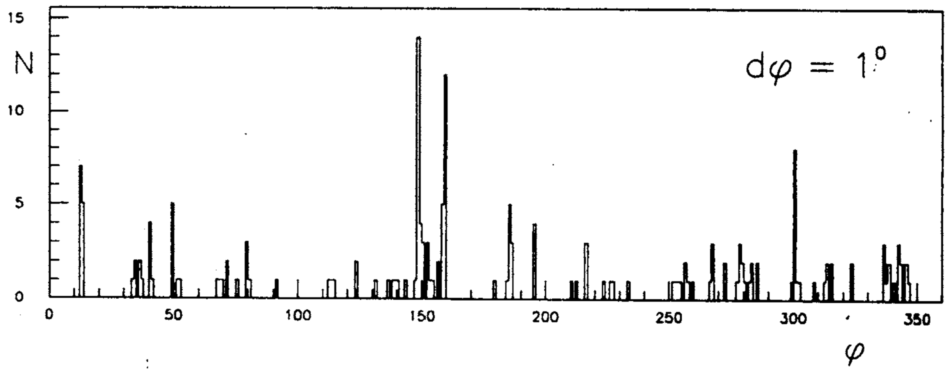

Fig.5. The energy deposited in the central 6 cm width ring of SMD vs. azimuthal angle for 6°, 3° and 1° per bin for the central AuAu collisions

2.2. π^0/γ *Separation.* We have, also, carried out a study of the separation of shower coming from single γ from those coming from a π^0 decay. In our calculation we considered a SMD with only one sensitive plane with the pad structure, described above. We used a procedure similar to the method, described in [3]. Three variables were used to find a coefficient of π^0 rejection for 90% γ acceptance:

— E — the energy deposited by the shower;

— r — the energy weighted shower radius;

— Er^2 — the energy dispersion of the shower.

The energy weighted centre of the shower is calculated as follows:

$$X_c = \sum_i x_i / \sum_i E_i ,$$

where E_i is the energy deposited in the ith pad and X_i is the position coordinate of the ith pad in the pad units. The energy weighted shower radius, r, is calculated as:

$$r = \sum_i D_i E_i / \sum_i E_i ,$$

where $D = |X_c - X_i|$ is the distance of the ith pad from the calculated centre of the shower. The energy dispersion of the shower is calculated as:

$$Er^2 = \sum_i E_i D_i^2 .$$

Figure 6 shows the scatter plot of the energy dispersion Er^2 vs. the wighted shower radius r for 100 showers initiated by 15 GeV γ's and π^0's in the middle part of the SMD (rapidity $\eta \approx 1.5$). The energy summation was taken over 15 pads in radial and 10 in azimuthal directions from calculated centre of the shower. The marked area in Fig.6a contains 90% of the single γ showers. In the scatter plot for π^0 initiated showers the area of 90% single γ efficiency is marked. The showers within this area are classified as showers initiated by γ's, while all showers outside this area — as π^0 initiated showers. The π^0 rejection efficiency is given by the percentage of π^0 initiated showers which are outside this area. In this case we have obtaned the π^0 rejection efficiency of 63%. The results of the similar calculations for the SMD with two sensitive plans consisted of 1 cm width scintillator strips are shown in Fig.7. The value of the π^0 rejection efficiency is 60% in this case. It is seen, that for the SMD with only one pad-type sensitive plane we get practically the same π^0/γ separation as for the SMD with two strip-type planes.

The future investigations are needed in this direction. In our opinion the information about the φ cooridnate from second SMD plane will significantly improve the efficiency of π^0/γ separation.

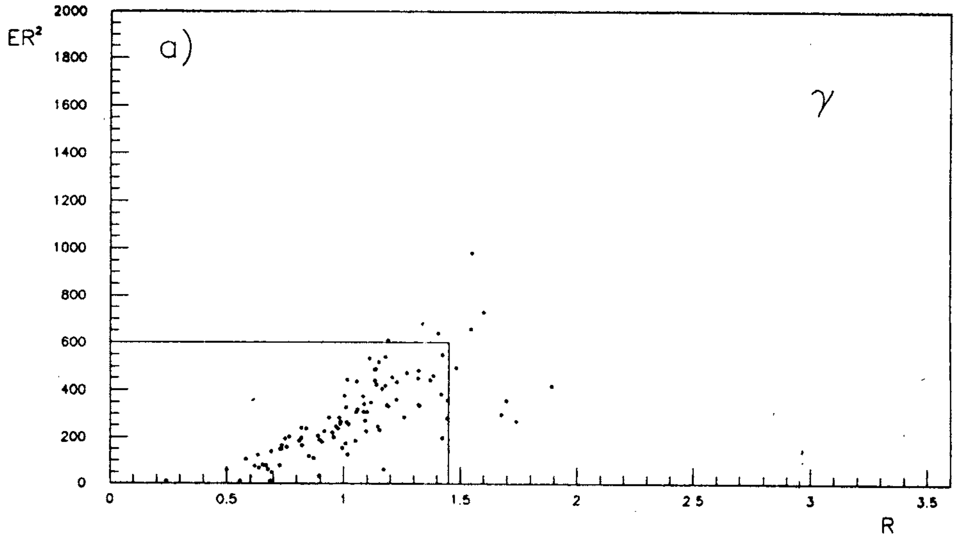

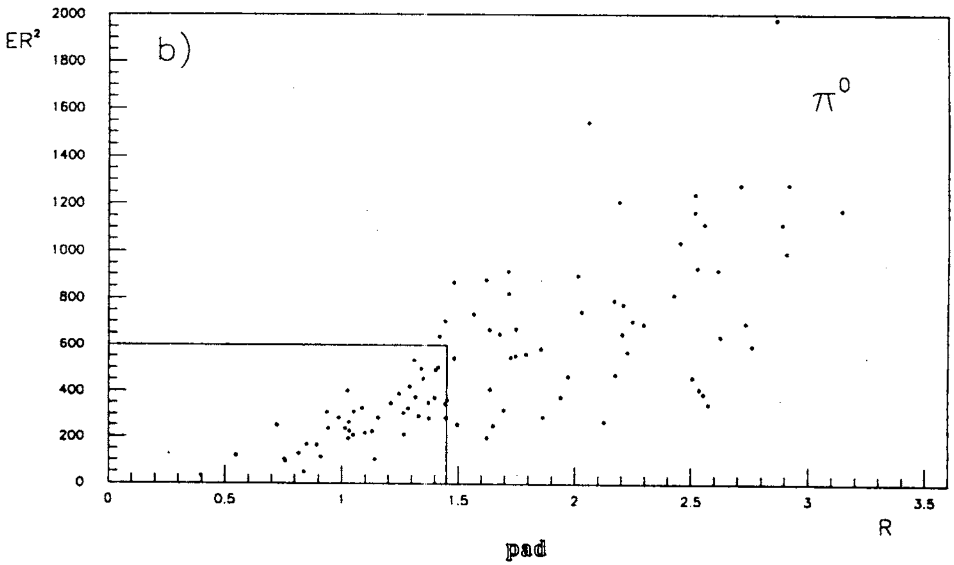

Fig.6. The scatter plot of sample of 15 GeV γ initiated showers as a function of the energy dispersion Er^2 and the weighted shower radius r for the SMD with one pad sensitive layer

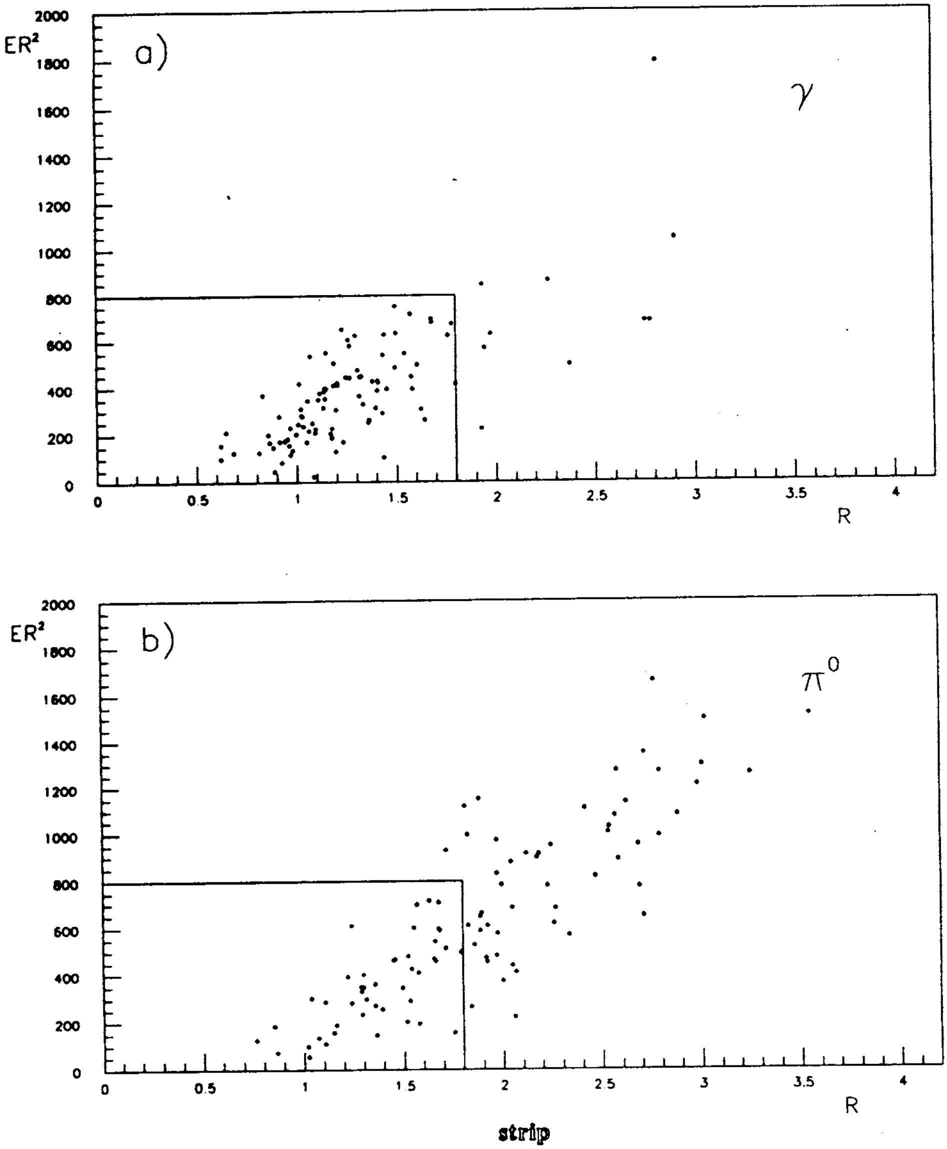

Fig.7. The same as in Fig.6 for the SMD with two strip sensitive layer

3. Conceptual Design

Following by the Monte Carlo calculation results we proposed to use as an option of SMD a thin multiwire gas chamber with analog readout of anode wires and of cathode pads to measure the position of EM showers. The analog readout is sensitive to the density of particles inside the shower, thus providing a localization of the shower core by a simple determination of the weighted centre in a cluster of signals. We adopt OPAL [4] and CDF [5] groups methods in our proposal. The thin multiwire gas chambers, operating in a satured mode, were used for electromagnetic presumpling in the endcaps of OPAL detector at LEP [4]. At Fermilab for the Collider Detector Facility the shower counter strip chambers were used operating with the gain of 10^4 [5].

The suggested SMD multiwire gas chamber will be CDF or OPAL-type chamber with pad structure of cathode as followed from MC simulations.

3.1. *Description of Detector.* Space and timing restrictions are the major concern for detector design. It is proposed that the SMD will be inserted into 25 mm gap into the endcap EMC at the depth of $5 \div 7X_0$. It will consist of 12 trapezoidal sectors each of which covers 30° azimuthal angle. The geometrical dimensions are given in Fig.8. A schematic view of the cross section of two chambers is shown in Fig.9 and Fig.10.

In the OPAL-type chamber (Fig.9) the anode wire plane consists of 637 gold coated tungsten W-Re wires of 30 μm diameter rounded on the supporting frame with space step of 2 mm in the direction along the sector axes line. Groups of five wires are then ORed. The wires strung with a tension of about $80 \div 100$ g. Long wires are supported every 60 cm by spacers to avoid sagging and to provide a mechanical strength for the chamber itself. The dead space loss due to this support is less than one per cent.

The CDF-type chamber (Fig.10) has a ribbed construction. Aluminum ribs profile will be producted using the extrusious technology. The anode wires are placed at the centre of cells with the step of 1 cm by means of special supporting plates. The individual anode wire is connected to high voltage by 1 MΩ resistor and readout through capacity of $200 \div 400$ pF.

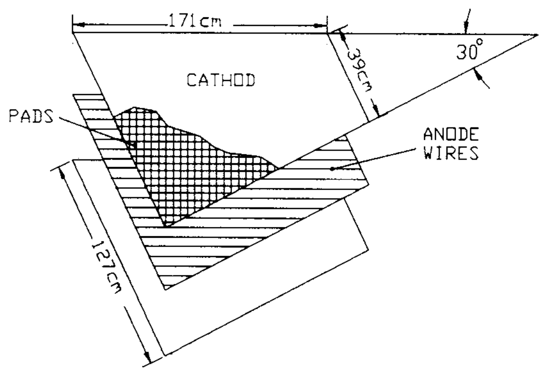

Fig.8. Layout and dimensions of the SMD multiwire gas chamber

The cathode planes of chambers are 1.5 mm thin G10 sheets of whose internal faces (forward wires) copper pads are formed by chemical etching.

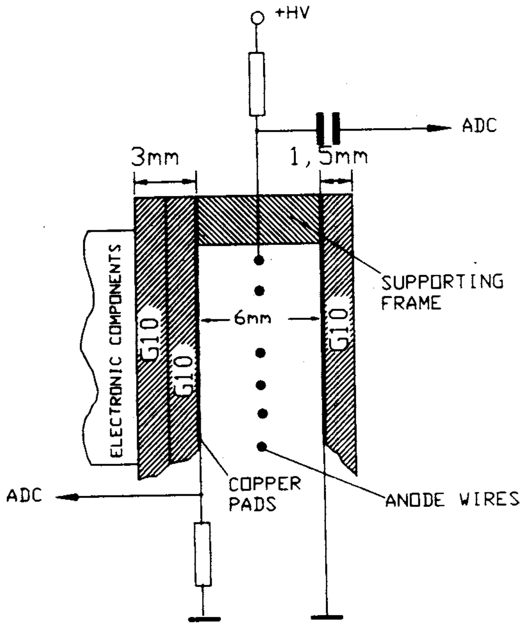

Fig.9. Schematic view of cross section of the OPAL-type SMD multiwire gas chamber

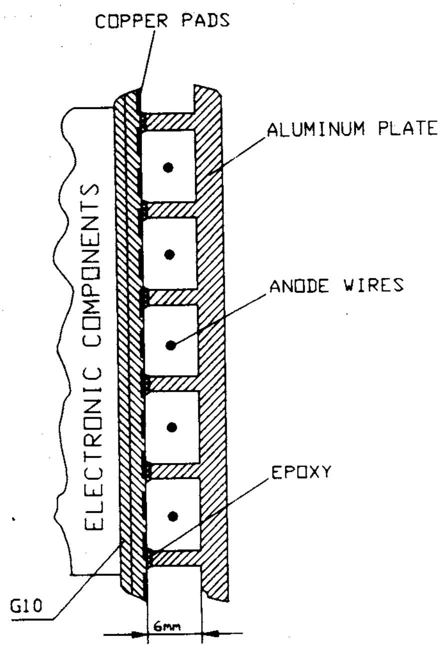

Fig.10. The same as in Fig.9 for the CDF type chamber

Following by the results of MC calculations it follows that there are 190 bins in radial and 10 bins in azimuthal directions, total — 1900 pads. The size of the pads decreases going towards the beam axes to resolve ambiguites due to increasing multiplicity. The cathode plane is placed at the distance of 3 mm from the anode wire plane.

The full cathode plane consists of a few pieces. These pieces are glued in turn to the face of G10 sheet to obtain the full cathode plane of the SMD sector. This cathode plane is glued to the ribs aluminum plate (CDF-type chamber) or pressed to the supporting frame (OPAL-type chamber). The outer face of cathode is used for readout electronics components. The gas mixture argon — DME or argon — CO_2 will be used.

3.2. *Readout Electronics.* The two space coordinates are provided by the simultaneous readout of wires pads. This results in a total 2027 electronic channels per sector and 24324 channels for full endcap SMD. All channels have multiplexing analog readout. The front end electronics is directly mounted onto the outer face of the cathode plane. A shielded TWP cable is used to transport the signals to the rear end. At the rear end additional multiplexing will be obtained in the ADC module. 12 bit charge sensitive ADC will be enough to cover a dynamic range from minimum ionizing particles up to showers.

4. Conclusion

Our Monte Carlo calculation results show that the Shower Maximum Detector with pad structure of sensitive layer has more suitable properties than the corresponding strip type especially in the case of investigation of the EM showers in the AuAu collision. Good position resolution and π^0/γ shower separation are realized even with only one sensitive SMD layer used. The estimates indicate that it is possible to build the SMD as a pad multiwire chamber which will have an acceptable cost.

5. Acknowledgements

The authors are grateful for support by the Russian Fundamental Science Foundation under grant 95-02-05061 and the RHIC Department at BNL under contract 776746.

References

1. Design and Study of Light Readout System for Scintillator Shower Maximum Detector for EMC Endcap. STAR Note 226, submitted to JINR Rapid Communications.
2. Akimenko S.A. et al. — IHEP Preprint 94-94, Serpukhov, 1994.

3. Grunhaus J., Kananov S., Milstene C. — Nucl. Instr. and Meth., 1995, A354, pp.368—375.
4. Beard C. et al. — Nucl. Instr. and Meth., 1990, A286, pp.117—127.
5. Nodulman L. — Nucl. Instr. and Meth., 1980, 176, pp.345—347;
Balka L. et al. — Nucl. Instr. and Meth., 1988, A267, pp.272—279.

Received on December 6, 1995.